Investigation of TiO_2 and TiO_2 /Zn Thin Films’ Optical and Structural Studies for Optoelectronic Devices

Prashant Meena
Department of Physics, Vivekananda Global University, Jagatpura

Pavan Kumar Meena
Department of Physics, Vivekananda Global University, Jagatpura

Sumit Sharma
Department of Mechanical Engineering, Poornima College of Engineering, Sitapura

Mukesh Didwania
Department of Mechanical Engineering, Poornima College of Engineering, Sitapura

他

https://doi.org/10.5109/7342437

出版情報：Evergreen. 12 (1), pp.41-49, 2025-03. 九州大学グリーンテクノロジー研究教育センター
バージョン：

Investigation of TiO_2 and TiO_2/Zn Thin Films' Optical and Structural Studies for Optoelectronic Devices

Prashant Meena[1], Pavan Kumar Meena[1], Sumit Sharma[2], Mukesh Didwania[2], M.K.Jangid[1,*]

[1]Department of Physics, Vivekananda Global University, Jagatpura, Jaipur, Rajasthan 303012, India

[2]Department of Mechanical Engineering, Poornima College of Engineering, Sitapura, Jaipur, Rajasthan 302022, India

*Author to whom correspondence should be addressed:
E-mail: maheshjangid2008@gmail.com, mahesh.jangid@vgu.ac.in

(Received August 17, 2024; Revised November 21, 2024; Accepted January 7, 2025).

Abstract: The radio frequency (RF) magnetron sputtering was used to deposit pure TiO_2 and TiO_2/Zn thin films onto glass substrates. Annealing of the obtained thin films was done at 200°C, 250°C, and 300°C in a tube furnace for one hour each to see the effect of annealing on their properties. The effect on the films' structure, optical characteristics, and morphologies due to annealing temperature were analyzed using Field Emission Scanning Electron Microscopy (FE-SEM), X-Ray Diffraction (XRD), UV-Vis spectroscopy, and Energy Dispersive X-Ray Spectrometry (EDS) in electron microscopy (FE-SEM). The films revealed XRD peaks for hkl values (101), (004), (111), (200), (211), and (220) at 2θ=25.2°, 37.19°, 41.25°, 47.57°, 55.0°, and 62.2° respectively of anatase phase. From XRD, it appears that pure anatase TiO_2 phase is being created and after Zn coating on TiO_2 the anatase phase remains unchanged. In UV-Vis measurements all samples show low absorbance in visible region with a pronounced absorption edge in the ultraviolet region. Zn coating resulted in an increased bandgap for the TiO_2 thin films due to alter in the electronic structure and crystallite size. Furthermore, the direct bandgap of the annealed samples were reduced with annealing temperatures for both the cases. The existence of homogeneous thin films was demonstrated by the FE-SEM characterization data. This work advances the growth of novel material for a large range of technical uses in optoelectronic device applications.

Keywords: Thin Film; Annealing; XRD; UV-Vis; FE-SEM; EDS

1. Introduction

Among the transparent conducting oxide (TCO) composites, TiO_2 stands out due to its non-toxic nature, chemical stability, and high refractive index[1)]. Thin layers are particularly valuable in optoelectronic devices because they exhibit enhanced physical characteristics compared to bulk materials[2)]. Numerous transition metals (TM) have been extensively researched[3,4)], including Co, Fe, Ag, Ni, and Mn, as well as oxides of doped metal semiconductors including TiO_2[5)], MgO[6)] and SnO_2[7,8)]. TiO_2, one of these metal oxides, have been studied extensively because of their great stability, low cost, and electrical and magnetic properties[9)]. TiO_2 thin films are utilized in different areas including electronics, optics, and medicine[10,11)]. TiO_2 is one of the semiconductor materials that has been studied the most[12,13)]. It is an inexpensive, chemically stable substance with exceptional semiconducting and catalytic qualities[14,15)]. Magneto-optoelectronic applications can be facilitated by tailoring the energy bandgap and enhancing saturation magnetization of nanostructured TiO_2 by appropriately doping during the preparation of thin films. These fields have pinched a lot of interest and have long been important study focuses[16,17)]. In the field of surface science pertaining to metal oxides, TiO_2 nanostructures have been the subject of the most extensive research[18)]. The bandgap 3.2 eV to 3.4 eV have been reported in the common TiO_2 with phases brookite, rutile, and anatase[19,20)]. The optical and structural characteristics of TiO_2 thin films can be significantly altered through the doping process with Co, Zn, Ni, and Mn[21,22)], promoting photocatalytic activity in the visible region, which enhances their potential for optoelectronic device applications[23,24)]. TiO_2 with Nb, Fe, and Zn in particular has been shown to be successful in changing its bandgap energy and making it active in visible light[25,26)]. Zn doping in TiO_2 modify its interfacial electron transfer, thereby enhancing its photoreactivity[27,28]. Improving the properties of TiO_2, including its conductivity and band gap, is essential for expanding its range of applications. Doping TiO_2 significantly alters its band structure and trap states[29,30]. However, the material's strong absorption in the UV region limits its responsiveness to visible light. To address this, metal doping has been employed to enhance TiO_2's ability to absorb visible light by reducing its band gap, thereby enabling photoactivity in the visible spectrum[31,32]. The impact of annealing treatment on their structural and optoelectronic properties have been analyzed and reported that annealed TiO_2 thin films exhibit improved crystallinity and larger grain sizes compared to their pristine counterparts, emphasizing the significance of annealing temperature in enhancing nanocrystal growth[33]. Furthermore, optoelectronic analyses revealed that annealed TiO_2 thin films possess a reduced band gap energy and exhibit enhanced optoelectronic activity[34,35].Due to oxygen deficiency, the doped TiO_2 semiconductor exhibits an intrinsic n-type property and a broad straight bandgap in the 2.96 -3.20 eV range[36,37].Furthermore, it has superior optoelectronic qualities[38]. Al doped TiO_2 thin films have been reported to evaluate their potential for optoelectronic applications. The effect of varying aluminum doping concentrations on the photovoltaic performance of solar cells was systematically examined and reported that incorporating aluminum into TiO_2 influences the crystal size of anatase TiO_2, resulting in smaller crystal sizes for the doped thin films compared to the undoped ones. Furthermore, doping improves the light absorption efficiency of TiO_2thin films by altering their electronic structure[39]. In this study, pure $TiO_2$and TiO_2/Zn thin films were investigated for optical and structural properties to make them suitable for use in optoelectronic device applications.

2. Experimental

The radio frequency (RF) magnetron sputtering technique was used to deposit pure $TiO_2$and TiO_2/Znthin films onto the glass substrates. Sputtering targets of TiO_2 (99.99%) and Zn (99.99%) of 10mm dia and 2 mm thickness were used to prepare the thin films. High-purity argon gas was employed for sputtering, and the argon pressure in the chamber was first set to 10^{-3} mbar for 15 minutes before deposition and maintained at 10^{-3} mbar during the process. The distance between the target and substrate was 140 mm, and the substrate was kept at room temperature. Plasma stability was ensured by using a standard RF frequency of 13.56 MHz, while the base pressure was held at 10^{-5} mbar to minimize contamination. The power setting of 50 Watt was used during the deposition process. Thin films of TiO_2 (200 nm) and TiO_2/Zn (300 nm) were deposited on glass substrates with deposition rates of 0.14 Å/s for TiO_2 and 0.63 Å/s for Zn. Subsequently, the prepared thin films underwent annealing in a programmable muffle furnace at 200°C, 250°C and 300°C temperatures for an hour. The XRD analysis of the samples was obtained using a Panalytical X-ray diffractometer. UV-Vis measurements of the films were taken by a UV-1800 Shimadzu spectrophotometer. The surface morphology and elemental composition were investigated using a Nova Nano Field Emission Scanning Electron Microscopy (FE-SEM) with Energy Dispersive X-Ray Spectrometry (EDS).

3. Results and Discussion

3.1 XRD Analysis

To observe the crystal structures of samples, their XRD pattern were analyzed using a Panalytical X-ray diffractometer. Figure1 presents the XRD pattern of pristine TiO_2 thin film. The diffraction peaks were observed at 2θ=25.2°, 37.19°, 41.25°, 47.57°, 55.0°, and 62.2°, with hkl values (101), (004), (111), (200), (211), and (220) respectively, as identified by JCPDS card no. 21-1272. The XRD result indicates that the pure TiO_2 films are polycrystalline, consisting solely of the anatase phase. This XRD pattern match perfectly with JCPDS card no. 21-1272, which is specific to the anatase phase of TiO_2. The presence of these distinct diffraction peaks confirms the crystallinity and phase purity[40].

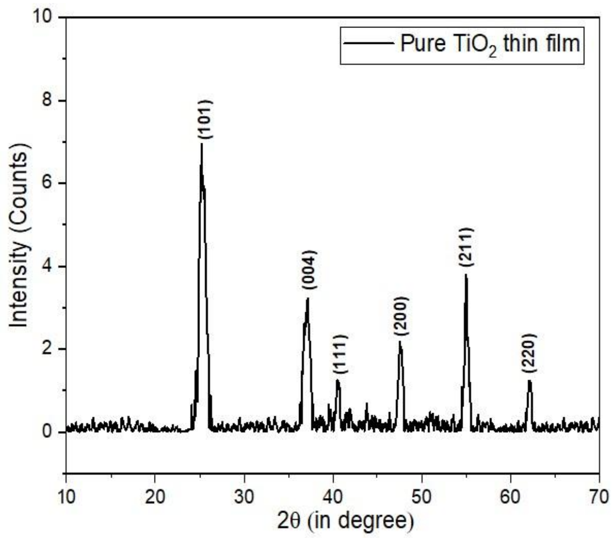

Fig. 1: XRD pattern of pristine TiO_2 thin film.

XRD pattern of TiO_2/Zn coated thin films for both cases (i) pristine and (ii) annealed (300°C) reveal significant insights into their crystal structure, as depicted in Fig. 2. To evaluate the crystal phase of these films, the samples were examined over a range of 10° to 90° using X-ray diffractometer. The XRD patterns demonstrate that the samples are crystalline, with distinct peaks related to the (101), (004), (200), (211), and (220) planes. These peaks are observed at 2θ=25.2°, 37.19°, 47.57°, 55.0°, and 62.2°, respectively. The diffraction pattern confirms that the thin films exhibit anatase phase of TiO_2. This is evident from the presence of the characteristic peaks in all samples. The XRD pattern for both the pristine and annealed samples are identical, indicating that annealing at 300°C does not alter the anatase phase of the TiO_2/Zn thin films. The absence of additional peaks indicates that the films are free from other phases or impurities, such as ZnO or other zinc-based compounds. This confirms the effective incorporation of Zn into the TiO_2 matrix while preserving the anatase structure. The XRD patterns of the annealed samples further indicate that these samples retain the anatase structure, suggesting that the annealing treatment at 300°C does not induce any significant structural changes. The consistent XRD patterns before and after annealing highlight the constancy of anatase phase in TiO_2/Zn thin films and demonstrating effectiveness of the RF magnetron sputtering technique in producing high-quality thin films. This stability is crucial for potential applications in optoelectronics, where maintaining a well-defined crystal structure is essential for optimal performance[41)].

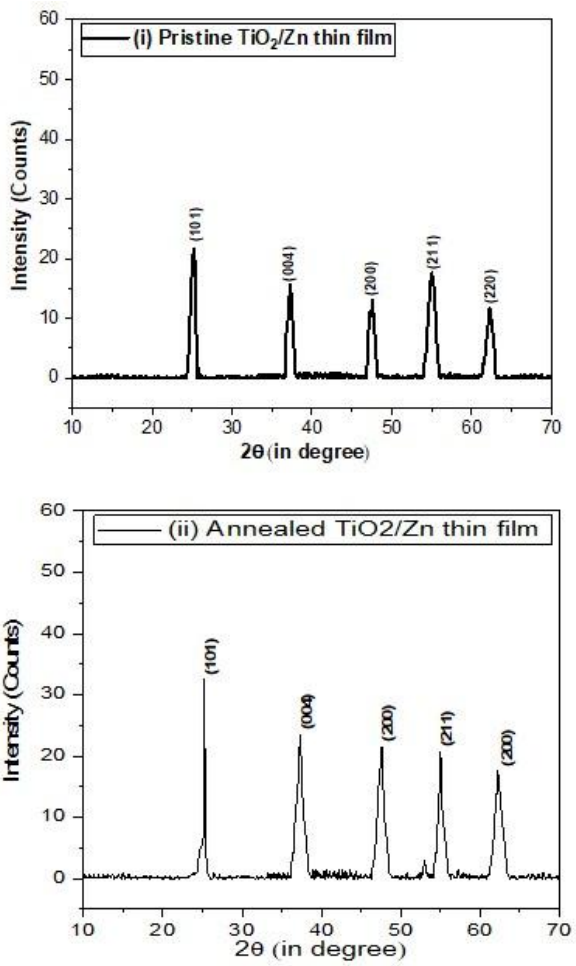

Fig. 2: XRD pattern of TiO_2/Zn thin films (i) Pristine, (ii) Annealed at 300°C.

The Scherrer formula[42)] was used to determine the average grain size (D) of the thin films.

$$D = \frac{K\lambda}{\beta cos\theta}$$

The Scherrer equation, where K is the Scherrer constant (K = 0.94), λ is the X-ray wavelength (λ=1.54 Å) θ is the Bragg diffraction angle, and β is the full width at half maximum (FWHM) of the principal XRD peak, was employed for analysis[43)]. It was observed that the incorporation of Zn into TiO_2influenced the crystal size of anatase TiO_2. Specifically, Zn-coated TiO_2 thin films exhibited smaller crystal sizes compared to pure TiO_2 thin films. The calculated crystal sizes for TiO_2 and TiO_2/Zn thin films were 27.65 nm and 18.63 nm, respectively, well agree with previously reported[44)]. This reduction in crystal size can be attributed to the quantum size effect, wherein the inclusion of Zn significantly decreases the crystal size. The most prominent XRD peak for pristine and annealed TiO_2/Zn thin films were observed at 2θ=25.2°. The results indicate that an increased in intensity and a reduced FWHM for annealed samples as compared to the pristine TiO_2/Zn thin films. This behavior indicates enhanced crystal growth and increased crystal size after annealing. The obtained FWHM value for the pristine TiO_2/Zn thin film 0.493, corresponding to an average crystal size of 18.63 nm and after annealing, the FWHM decreased to 0.294, resulting in an average crystal size of 27.79 nm. These findings highlight the critical role of annealing temperature in improving the crystal size of TiO_2/Zn thin films.

3.2 UV-Vis Analysis

Figure3 illustrates the absorption spectra of (i) pure TiO_2 (ii) TiO_2/Zn thin films. It was observed that the absorbance for both thin films is very low in the visible region, indicating that these films are transparent to visible light. This transparency is advantageous for applications requiring optical clarity, such as protective coatings or transparent conductors. A strong absorption edge is observed in the ultraviolet region for both types of films, which may be endorsed to the bandgap absorption of TiO_2. The presence of this sharp absorption edge is characteristic of the electronic structure of TiO_2, where ultraviolet (UV) light absorption causes electrons to shift from valence to conduction band[45,46)]. Moreover, the absorption spectra reveal that the absorbance decreases with increasing annealing temperature for both the cases. It may be due to improved crystallinity and reduced defect density. These are well agreeing with XRD analysis. The film crystallinity improves, leading to a reduction in the number of defects and, consequently, lower absorbance[47,48)]. This phenomenon suggests that annealing enhances the optical quality of the films, making them more suitable for applications that require high optical transparency and low defect densities, such as in optoelectronic devices. The UV–Visible absorption analysis thus provides crucial insights and demonstrating their potential for various technological applications. The transparency in Vis-region and distinct absorption edge in the UV-region, highlight their suitability for applications in UV detectors, photocatalysis, and solar cells. Furthermore, the improvement in optical properties with annealing underscores the importance of thermal treatment in optimizing the performance of the films[49,50].

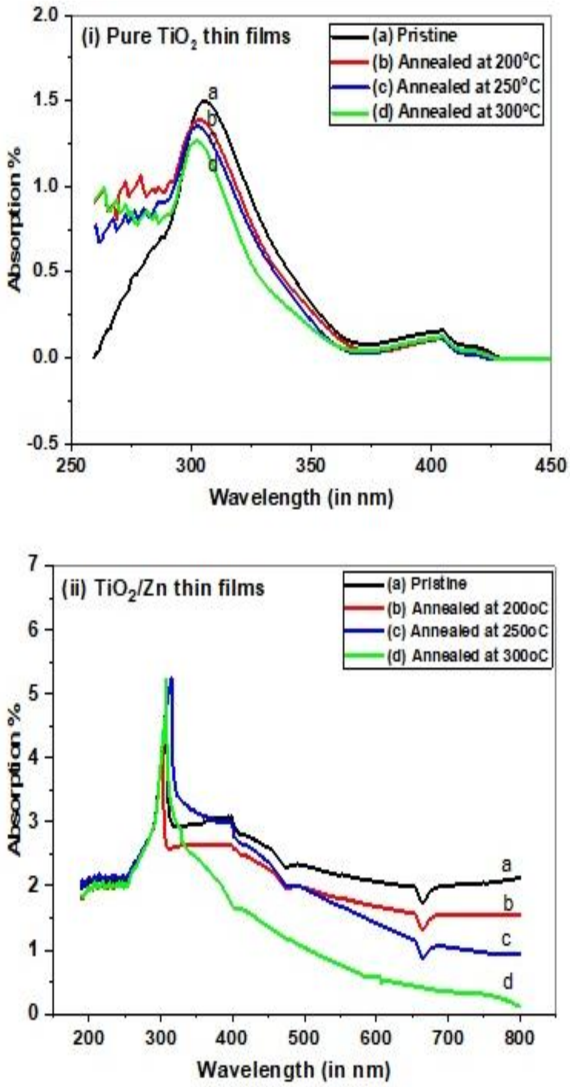

Fig. 3: Absorption spectra of (i) pure TiO_2, (ii) TiO_2/Zn thin films.

The optical bandgap (Eg) of samples was determined by Tauc's relation:

$$\alpha h\nu = (h\upsilon - E_g)^n$$

where α represents the absorption coefficient, hν is the photon energy, and A is a constant known as Tauc parameter. For direct bandgap, n equals 0.5, whereas for indirect bandgap, n equals 2[51,52]. Figure4 illustrates the tauc plots for both pure $TiO_2$and TiO_2/Znfilms. The optical bandgap is found by extending the linear. segment of this plot to intersect the energy axis. The analysis indicates that the bandgap decreases with increasing annealing temperature for both the cases (Table1). This decrease is primarily endorsed to increase the grain size and the reduction of internal stress within the films due to the annealing process[53,54]. As the grain size grows, the quantum confinement effects are reduced, leading to a narrower band gap. Also, annealing can induce the formation of oxygen vacancies, introducing new electronic states near the conduction level and further reducing the bandgap energy. Also the results illustrate that the bandgap of TiO_2/Zn thin films are slightly higher than the pure TiO_2 thin films (Table1). These results can be explained by the alteration in the electronic structure. The variation in crystallite size brought about by the addition of zinc is also accountable for that. The addition of Zn atoms creates new energy states and reduces defect density, leading to a wider bandgap. This action is consistent with the Burstein-Moss effect, in which the bandgap seen in optical measurements is essentially widened as a result of the Fermi level shifting into the conduction band, effectively widening the band gap observed in optical measurements. The Burstein-Moss effect occurs because the added electrons from the Zn dopant increase the carrier concentration, filling the lower energy levels in the conduction band. As a result, the absorption edge moves to higher energies, effectively increasing the optical bandgap. This shift can also be explained by the presence of charged defects. The charged defects generated by Zn doping might be neutralized by other defects, resulting in an overall raise in bandgap. The results of this study align with previous research that has demonstrated the modulation of bandgap energy levels in metal oxide thin films through metal ion doping[55].

Table 1. Optical energy bandgap of pure TiO_2 and TiO_2/Zn thin films with annealing temperature.

Annealing Temperature	Energy Bandgap (in eV)	
	TiO_2	TiO_2/Zn
Pristine	3.81	4.10
200°C	3.76	4.03
250°C	3.73	3.94
300°C	3.71	3.78

The variationin the bandgap by doping is a crucial aspect for customizing optical characteristics of films for specific uses such as photocatalysis, and optoelectronics. The ability to control the bandgap through annealing and doping provides a valuable means for optimizing the performance of these materials in different applications. For instance, a narrower band gap can enhance the photocatalytic of TiO_2 by extending its absorption into the vis-region of the spectrum. This is particularly important for solar energy conversion. Moreover, the improved crystallinity and reduced defect density achieved through annealing are essential for the stability and efficiency of optoelectronic devices. High-quality thin films with fewer defects are less likely to suffer from recombination losses, thereby improving the performance of solar cells and light-emitting diodes[56,57].

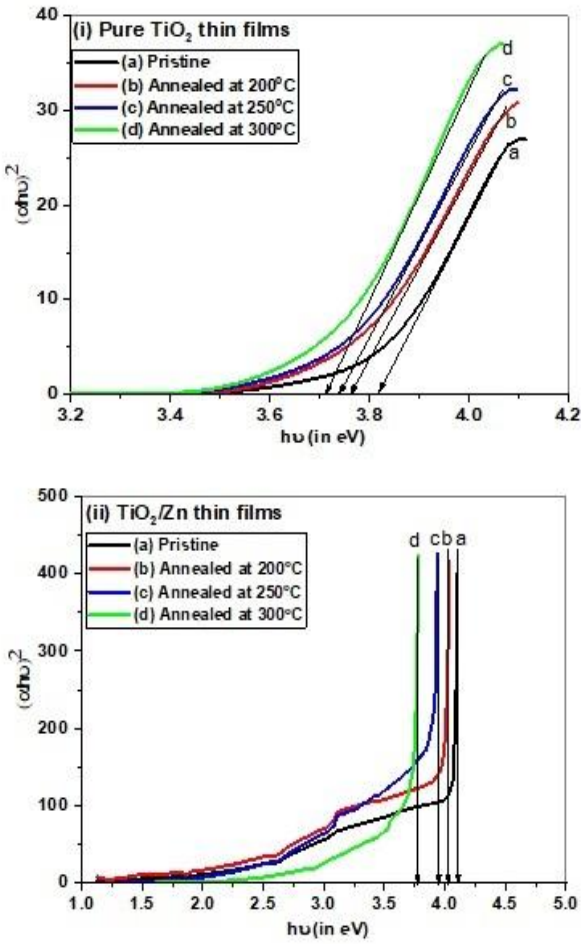

Fig. 4: Tauc spectra of (i) pure TiO_2, (ii) TiO_2/Zn thin films.

3.3 FE-SEM and EDS Analysis

Figure5 presents the FE-SEM images of the pure TiO_2 thin film, captured at different magnifications of 2, 3, 4, and 10 µm. FE-SEM provides detailed images of the surface structure, revealing the nanostructured morphology of thin films. The images demonstrate a uniform distribution of particles with high crystallinity. The films's surface appears smooth and dense, with no visible cracks or defects, which are essential for its application in various technologies. To further understand the elemental composition of the nanostructures, EDS measurements were conducted. Figure6 shows EDS spectra of pure TiO_2 thin film, indicating the existence of Ti and O as the primary elements. Table 2 summarizes the elemental composition, confirming that the thin films consist predominantly of Ti and O, which aligns with the expected stoichiometry of TiO_2. The uniform and defect-free morphology observed in the FE-SEM images suggests that the synthesis method employed is effective in producing high-quality thin films. The existence of Ti and O only in EDS spectra further confirms the purity of the samples, with no detectable impurities. In many cases, the properties and performance of thin films are heavily influenced by their surface morphology. For instance, in optoelectronic devices, a smooth, defect-free surface facilitates efficient charge transport and reduces recombination losses, ultimately enhancing the overall performance of the device[58,59].

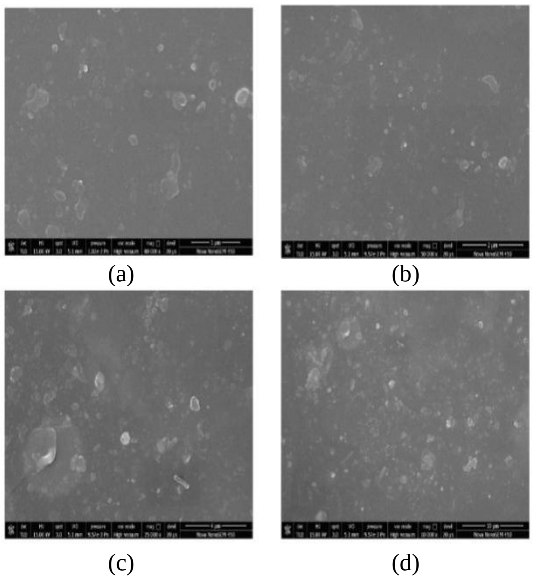

Fig. 5: FE-SEM images of the pure TiO_2 thin film, captured at different magnifications of (a) 2, (b) 3, (c) 4, (d) 10µm.

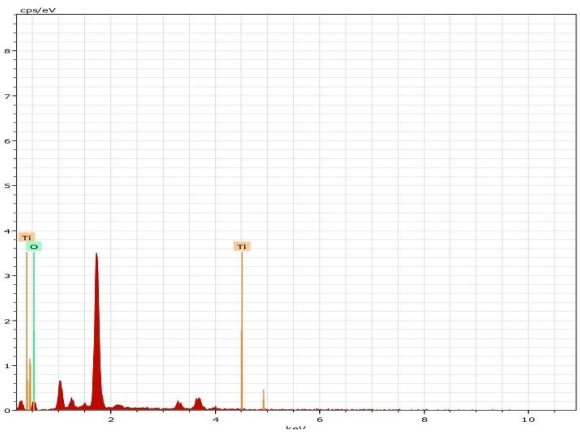

Fig. 6: EDS spectra of pure TiO_2 thin film.

Table 2. Elemental composition of pure TiO_2 thin films.

Element	Atomic Number	Unn. C [wt.%]	Norm. C [wt.%]	Atom. [at.%]	C Error (1 Sigma) wt.%]
O	8	91.30	91.30	96.92	30.73
Ti	22	8.70	8.70	3.08	1.73
Total		100.00	100.00	100.00	

4. Conclusion

The XRD investigation of the thin films confirmed the formation of TiO_2 anatase phase, as evidenced by the diffraction peaks related to planes (101), (111), (004), (200), (211), and (220) of the anatase lattice. The intensity of these anatase peaks showed a slight increase after annealing, indicating improved crystallinity. The films exhibited optical absorption consistent with their bandgap energy. The strong absorption edge in the UV-region and transparency in the vis-region highlight the potential of these films for UV detectors, and solar cells. The decrease in absorption with increasing annealing temperature further underscores the importance of thermal treatment in enhancing the optical quality of films. The optical analysis revealed that the direct bandgap of TiO_2/Zn thin films is slightly high in respect to pure TiO_2 thin films. In addition, the bandgap decreases with increasing annealing temperature for both pure $TiO_2$and TiO_2/Zn thin films. The observed decrease in bandgap with higher annealing temperatures can be attributed to an increase in grain size and a reduction in internal stress within the films. These changes reduce quantum confinement effects, as larger grains transition away from the confinement regime. Furthermore, the elevated annealing temperatures facilitate the formation of oxygen vacancies, which create defect states near the conduction band. These new electronic states can narrow the bandgap by enabling additional pathways for electronic transitions; these factors contribute to the observed variations in the electronic properties of the films. FE-SEM and EDS analyses confirmed the uniformity and presence of elements in the thin films.In conclusion, this study demonstrates that the prepared thin films exhibit considerable potential for a range of optoelectronic applications. Notably, annealing within the temperature range of 200°C to 300°C was found to optimize their optoelectronic performance, highlighting this process as a critical factor in enhancing material properties for practical applications.

Acknowledgements

The authors specially (Prashant Meena) are highly thankful to UGC for providing financial support under JRF scheme for this work. They would also like to acknowledge the Material Research Centre, MNIT Jaipur Department of Physics, University of Rajasthan, Jaipur to provide experimental facilities for this research.

Nomenclature

XRD	X-Ray. Diffraction
UV-Vis	Ultraviolet Visible
TiO2	Titanium Dioxide
Zn	Zinc
FE-SEM	Field Emission Scanning. Electron Microscopy

References

1) K. Taira, and H. Einaga, “Distribution ratio of Pt on anatase and rutile TiO2 particles, determined by X-ray diffraction and transmission electron miscroscopy analysis of Pt/TiO2(P25),” *Evergreen*, 5 *(4)* 13-17 (2018). doi:10.5109/2174853.
2) L. Al-Salem, and R. Seoudi, "Effect of annealing on the structural properties of TiO2 thin films," *Journal of Materials Science: Materials in Electronics*, 31 22642-22651 (2020). doi：10.1007/s10854-020-04223-0.
3) A. Fauzi, L.H. Lalasari, N. Sofyan, A. Ferdiansyah, D. Dhaneswara, and A.H. Yuwono, “Titanium dioxide nanosheets derived from Indonesian ilmenite mineral through post-hydrothermal process,” *Evergreen*, 9*(2)* 470-475 (2022). doi:10.5109/4794174.
4) R.S. Ganesh, Aamir Y. Mamajiwala, E. Durgadevi, M. Navaneethan, S. Ponnusamy, C.Y. Kong, C. Muthamizhchelvan, Y. Shimura, and Y. Hayakawa, "Photocatalytic activity of TiO2 thin films," *Materials Chemistry and Physics*, 234 259-267 (2019).doi:10.1016/j.matchemphys.2019.05.045.
5) B. Santara, B. Pal, and P. K. Giri, “Signature of strong ferromagnetism and optical properties of Co doped TiO_2 nanoparticles,” *J. Appl. Phys.* 110, 114322 (2011). doi:10.1063/1.3665883.
6) M.K. Jangid, S.S. Sharma, J. Ray, Deepak Kumar, and Chagan Lal, "Structural, Optical and Electrical Characterizations of Mg/Ti/Ni multilayer thin films deposited by DC magnetron sputtering for hydrogen storage," *International Journal of Hydrogen Energy*, 48 37921-3799 (2022). doi:10.1016/j.ijhydene.2022.11.324.
7) S. Nurdin, Motlan, and M. Sirait, “Synthesis of ZnO Thin Film by Electroplating: Effect of Zinc Concentration on the Structural and Optical Properties,” *Evergreen*, 10*(2)* 715-721 (2023). doi:10.5109/6792820.
8) H.A. Shittu, O. Adedokun, M.A. Kareem, P. Sivaprakash, I.T. Bello, and S. Arumugam, "Effect of low-doping concentration on silver-doped SnO2," *Biointerface Research in Applied Chemistry*, 13 1-15 (2023). do:10.33263/BRIAC132.165.
9) K. Dodge, J. Chess, J. Eixenberger, G. Alanko, C. B. Hanna, and A. Punnoose, “Role of oxygen defects on the magnetic properties of ultra-small $Sn_{1-x}Fe_xO_2$ nanoparticles,” *J. Appl. Phys.* 113, 17B504 (2013). doi:10.1063/1.4794140.
10) A. Azani, D.S.C. Halin, M.M.A.B. Abdullah, K.A. Razak, M.F.S.A. Razak, M.M. Ramli, M.A.A.M. Salleh, and V. Chobpattana, “The effect of GO/TiO2 thin film during photodegradation of methylene blue

dye," *Evergreen*, 8*(3)* 556-564 (2021). doi:10.5109/4491643.

11) R. Vidhya, R. Gandhimathi, M. Sankareswari, P. Malliga, J. Jeya, and K. Neivasagam, "Nanostructured TiO2 thin films," *Journal of Nanostructures,*8*(3)* 232-241 (2018). doi:10.22052/jns.2018.03.004.
12) I. Ali, M. Suhail, A. Zied, Z.A. Alothaman, and A. Alwarthan, "TiO2 nanostructures: Properties and applications," *RSC Advances*, 8 30125-30147 (2018). doi:10.1039/C8RA06517A.
13) M. T. Sarode, P. N. Shelke, S. D. Gunjal, Y. B. Khollam, M. G. Takwale, S. R. Jadkar, B. B. Kale, and K. C. Mohite, "Effect of annealing temperature on optical properties of titanium dioxide thin films prepared by sol-gel method," *Int. J. Mod. Phys. Conf. Ser.* 6, 13-18 (2012). doi:10.1142/S2010194512002863.
14) J. Gajendiran, and V. Rajendran, "Synthesis and characterization of coupled semiconductor metal-oxide (ZnO/CuO) nanocomposite," *Materials Letters*, 116 311-313 (2014). doi:10.1016/j.matlet.2013.11.063.
15) X. Liu, J. Iocozzia, Y. Wang, X. Cui, Y. Chen, Z. Li, and Z. Lin, "Noble metal-metal oxide nanohybrids with tailored nanostructures for efficient solar energy conversion, photocatalysis, and environmental remediation," *Energy Environ. Sci*, 10 402-434 (2017). doi:10.1039/C6EE02265K.
16) V.R. Akshay, B. Arun, G. Mandal, and M. Vasundhara, "Optical and magnetic behavior of Ni-doped TiO2 nanocrystals," *Physical Chemistry Chemical Physics*, 21 2519-2532 (2019). doi:10.1039/c8cp06875e.
17) G. A. Alamu, O. Adedokun, I. T. Bello, and Y. K. Sanusi, "Plasmonic enhancement of visible light absorption in Ag-TiO_2 based dye-sensitized solar cells," *Chem. Phys. Impact* 3, 100037 (2021). doi:10.1016/j.chphi.2021.100037.
18) A. T. Montoya, and E. G. Gillan, "Enhanced photocatalytic hydrogen evolution from transition-metal surface-modified TiO2," *ACS Omega* 3(3), 2947–2955 (2018). doi: 10.1021/acsomega.7b02021
19) B. Ünlü, and M. Ozacar, "Photocatalytic performance of TiO2 thin films," *Solar Energy*, 196 448-456 (2020). doi:10.1016/j.solener.2020.03.031.
20) Y. Alaya, R. Souissi, M. Toumi, M. Madani, L. El Mir, N. Bouguila, and S. Alaya, "Annealing effect on the physical properties of TiO2 thin films deposited by spray pyrolysis," *RSC Adv.*, 13*(32)* 21852-21860 (2023). doi:10.1039/d3ra02387g.
21) A. Zainal, S. Hadi, B. Sutanto, and D. Widhiyanuriyawan. "Investigation of Curcumin and Chlorophyll as Mixed Natural Dyes to Improve the Performance of Dye-Sensitized Solar Cells," *Evergreen*, 9*(1)* 17-22 (2022). doi:10. 5109/4774212.
22) Gupta, Gaurav, R. K. Tyagi, and S. K. Rajput. "A Statistical Analysis of Sputtering Parameters on Superconducting Properties of Niobium Thin Film," *Evergreen*, 8*(1)* 44-50 (2021). doi:10.5109/ 4372259.
23) S.A. Ahmed, "Annealing effects on Mn-doped TiO2," *Journal of Magnetism and Magnetic Materials*, 402 178-183 (2016). doi:10.1016/j.jmmm.2015.11.065.
24) A.S. Rini, R. Yolanda, F. Raysa, and F. Rakhmawati, "Improved Photocatalytic Activity of ZnO Film Prepared via Green Synthesis Method Using Red Watermelon Rind Extract," *Evergreen*, 9*(4)* 1046-1055 (2022). doi:10.5109/6625718.
25) M.K.Jangid, Sumit Sharma, Ved Prakash Meena, Ved Prakash Arya, and S.S. Sharma, "Impact of Annealing and Hydrogenation on the Optical Characteristics of ZnSe/Mn and ZnSe/Co DMS Thin Films Prepared via Thermal Evaporation Method" *Evergreen* 11*(1)* 178-185 (2024). doi:10.5109/7172253.
26) A. Yildiz, S. B. Lisesivdin, M. Kasap, and D. Mardare, "Electrical properties of TiO2 thin films," *J. Non-Cryst. Solids* 354(45-46), 4944-4947 (2008). doi:10.1016/j.jnoncrysol.2008.07.009.
27) D. Jiang, T. A. Otitoju, Y. Ouyang, N. F. Shoparwe, S. Wang, A. Zhang, and S. Li, "A review on metal ions modified TiO2 for photocatalytic degradation of organic pollutants," *Catalysts* 11(9), 1039 (2021). doi:10.3390/catal11091039.
28) J. Wang, X. Li, Y. Ren, Z. Xia, H. Wang, W. Jiang, C. Liu, S. Zhang, Z. Li, S. Wu, N. Wang, G. Liu, S. Liu, W. Ding, and Z. Zhang, "The effects of additive on properties of Fe doped TiO2 nanoparticles by modified sol-gel method," *J. Alloys Compd*. 858, 157726 (2021). doi:10.1016/j.jallcom.2020.157726.
29) S. Prabakaran, K. D. Nisha, S. Harish, J. Archana, M. Navaneethan, S. Ponnusamy, C. Muthamizhchelvan, and Y. Hayakawa, "Effect of Al doping on the electrical and optical properties of TiO2embedded graphene oxide nanosheets for optoelectronic applications," *Applied Surface Science*, 449, 332–339 (2018). doi:10.1016/j.apsusc.2018.03.234.
30) M. M. Abbas and M. Rasheed, "Solid state reaction synthesis and characterization of Cu doped TiO2 nanomaterials," *J. Phys.: Conf. Ser.* 1795, 012059 (2021). doi:10.1088/1742-6596/1795/1/012059.
31) M.-C. Wu, J.-S. Chih, and W.-K. Huang, "Bismuth doping effect on TiO2 nanofibres for morphological change and photocatalytic performance," *CrystEngComm*, 16, 10692–10699 (2014). doi:10.1039/c4ce01048a.
32) C. B. Anucha, I. Altin, E. Bacaksiz, and V. N. Stathopoulos, "Titanium dioxide (TiO2)-based photocatalyst materials activity enhancement for contaminants of emerging concern (CECs) degradation: In the light of modification strategies,"

Chem. Eng. J. Adv. 10, 100262 (2022). doi:10.1016/j.ceja.2022.100262.

33) M. I. El-Henawey, M. Kubas, A. El-Shaer, and E. Salim, "The effect of post-annealing treatment on the structural and optoelectronic properties of solution-processed TiO_2 thin films," *Journal of Materials Science: Materials in Electronics*, 32 (8), 9965–9975 (2021). doi:10.1007/s10854-021-06633-8.
34) R. K. Patnaik and N. Divya, "A brief review on the synthesis of TiO2_22 thin films and its application in dye degradation," *Materials Today: Proceedings*, 72, 2749–2756 (2023). doi:10.1016/j.matpr.2022.10.064.
35) Z. S. Hosseini, F. Haghparast, A. A. Masoudi, and A. Mortezaali, "Enhanced visible photocatalytic performance of un-doped TiO_2 nanoparticles thin films through modifying the substrate surface roughness," *Mater. Chem. Phys*. 279, 125530 (2022). doi:10.1016/j.matchemphys.2021.125530.
36) A. S. Keiteb, E. Saion, A. Zakaria, N. Soltani, and N. Abdullahi, "A modified thermal treatment method for the up-scalable synthesis of size-controlled nanocrystalline titania," *Appl. Sci.* 6(10), 295 (2016). doi:10.3390/app6100295.
37) J. Tao, X. Hu, J. Xue, Y. Wang, G. Weng, S. Chen, Z. Zhu, and J. Chu, "Structural and optical properties of TiO2 thin films for solar energy applications," *Solar Energy Materials and Solar Cells*, 197 1-6 (2019). doi:10.1016/j.solmat.2019.01.001.
38) G. Williams, B. Seger, and P.V. Kamat, "TiO2-graphene nanocomposites. UV-assisted photocatalytic reduction of graphene oxide," *ACS Nano*,2 1487-1491 (2008). doi:10.1021/nn800251f.
39) M. I. El-Henawey, M. Kubas, A. H. Oraby, A. El-Shaer, M. Abdelfatah, and H. Y. Salah, "Investigating the influence of Al2O3 doping on TiO2 optoelectronic properties and charge separation efficiency," *Opt. Mater.* 156, 115955 (2024). doi:10.1016/j.optmat.2024.115955.
40) X. Zheng, D. Zhang, Y. Gao, Y. Wu, Q. Liu, and X. Zhu, "Synthesis and characterization of cubic Ag/TiO2 nanocomposites for the photocatalytic degradation of methyl orange in aqueous solutions," *Inorg. Chem. Commun.* 110, 107589 (2019). doi:10.1016/j.inoche.2019.107589.
41) T. C. Paul, and J. Podder, "Synthesis and characterization of Zn-incorporated TiO2 thin films: impact of crystallite size on X-ray line broadening and bandgap tuning," *Appl. Phys. A* 125, 818 (2019). doi:10.1007/s00339-019-3112-9.
42) L. Ntozakhe, R. T. Taziwa, and H. H. Mungondori, "Influence of nitrogen doping on TiO2 nanoparticles synthesized by pneumatic spray pyrolysis method," *Mater. Res. Express* 6(8), 0850a9 (2019). doi:10.1088/2053-1591/ab2260.
43) M. Abdelfatah, A. Basuni, H. Y. Salah, M. Bakry, N. Darwesh, W. Ismail, and A. El-Shaer, "Improvement of physical and electrochemical properties of Cu2O thin films with Fe ions doping towards optoelectronic applications," *Opt. Mater.* 130, 112583 (2022). doi:10.1016/j.optmat.2022.112583.
44) U. O. A. Arıer and F. Z. Tepehan, "Influence of Al2 O3:TiO2 ratio on the structural and optical properties of TiO2-Al2O3 nano-composite films produced by the sol-gel method," *Composites Part B: Engineering*, 58, 147–151 (2014). doi:10.1016/j.compositesb.2013.10.016.
45) C. Yang, H. Fan, Y. Xi, J. Chen, and Z. Li, "Effects of Depositing Temperatures on Structure and Optical Properties of TiO2 Film Deposited by Ion Beam Assisted Electron Beam Evaporation," *Appl. Surf. Sci.*,254 2685-2689 (2008). doi:10.1016/j.apsusc.2007.10.006.
46) M.K. Jangid, and M. Singh, "Hydrogenation and annealing effect on electrical properties of nanostructured Mg/Mn bilayer thin films," *International Journal of Hydrogen Energy*, 37 3786-3791 (2012). doi:10.1016/j.ijhydene.2011.05.116.
47) M.K. Jangid, S.S. Sharma, J. Ray, and S.K. Jangid, "Effect of annealing and hydrogenation on optical and electrical properties of DC sputtered Mg-Ni Bilayer thin films," *Materials Today: Proceedings*, 67 847-851 (2022). doi:10.1016/j.matpr.2022.07.207.
48) M.K. Jangid, S.S. Sharma, and J. Ray, "Study on electrical, structural properties and hydriding kinetics of Mg/Al thin films," *Solid State Phenomena*338 83-90 (2022). doi:10.4028/p-m4rfxk.
49) T.M. Wang, S.K. Zheng, W.C. Hao, and C. Wang, "Studies on Photocatalytic Activity and Transmittance Spectra of TiO2 Thin Films Prepared by RF Magnetron Sputtering Method," *Surf. Coat. Technol.*,155 141-145 (2002). doi:10.1016/s0257-8972(02)00004-x.
50) M.K. Jangid, S.P. Nehra, and M. Singh, "Optical, electrical and raman properties of annealed hydrogenated Mg/Co bilayer thin films," *Journal of Nano- and Electronic Physics*,3 460-468 (2011).
51) Syed Mansoor Ali, Syed Tajammul Hussain, Jan Muhammad, M. Ashraf, Aslam Farooq, M. Imran, and Shahzad Abu Bakar, "Influence of magnesium doping on the structural and optical properties of tin (II) oxide thin films deposited by electron beam evaporation," *Materials Science in Semiconductor Processing*,16*(3)* 899-904 (2013). doi:10.1016/j.mssp.2013.01.017.
52) M.K. Jangid, S.S. Sharma, D. Mathur, and Y.C. Sharma, "Optical, Electrical and structural study of Mg/Ti bilayer thin film for hydrogen storage applications," *Materials Letters X*, 10 100076 (2021). doi:10.1016/j.mlblux.2021.100076.

53) M.K. Jangid, S.P. Nehra, and M. Singh, "Preparation and Characterization of Mg/Mn Bilayer Metal Hydrides Thin Films," *American Institute of Physics*, 1393 311-312 (2011). doi:10.1063/1.3653734.
54) M.K. Jangid, and S.K. Jangid, "Structural, electrical and optical properties of Mg-Ni thin films for hydrogen storage applications," *Trends in Sciences*, 19*(23)* 2067 (2022). doi:10.48048/tis.2022.2067.
55) M. Muñoz, F. H. Pollak, M. Kahn, D. Ritter, L. Kronik, and G. M. Cohen, "Burstein-Moss shift of n-doped In0.53 Ga0.47 As/InP," *Phys. Rev.* B 63, 233302 (2001). doi:10.1103/PhysRevB.63.233302.
56) M.K. Jangid, S.P. Nehra, and M. Singh, "Hydrogenation Effect on Mg/Mn Multilayer Thin Films," *American Institute of Physics*, 1349 685-686 (2011). doi:10.1063/1.3606043.
57) M. Ahamed, M. Khan, and M. Akhtar, "Role of Zn doping in oxidative stress mediated cytotoxicity of TiO2 nanoparticles in human breast cancer MCF-7 cells," *Sci. Rep*. 6, 30196 (2016). doi:10.1038/srep30196.
58) K. Albaidani, A. Timoumi, W. Belhadj, S.N. Alamri, and Saleh A. Ahmed, "Structural, electronic and optical characteristics of TiO2 and Cu-TiO2 thin films produced by sol-gel spin coating," *Ceramics International*, 49 36265-36275 (2023). doi:10.1016/j.ceramint.2023.08.309.
59) O. Adedokun, P. Sivaprakash, A.S. Ajani, I.T. Bello, and S. Arumugam, "Structural, optical and magnetic studies of sol-gel synthesized Mg-doped pure anatase TiO2 nanoparticles for spintronic and optoelectronics applications," *Physica B*, 667 415199 (2023). doi:10.1016/j.physb.2023.415199.